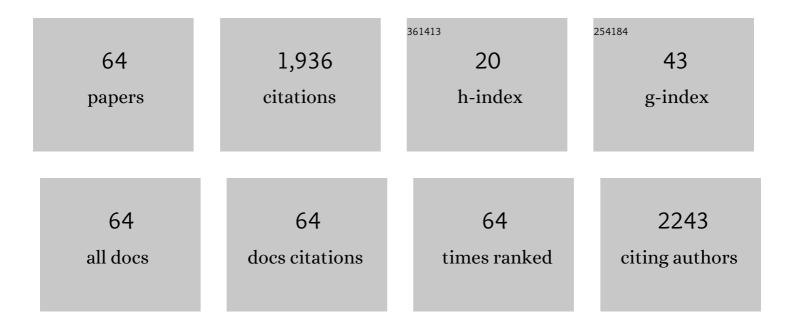
Xiaosong Zhou

List of Publications by Year in descending order

Source: https://exaly.com/author-pdf/8570624/publications.pdf Version: 2024-02-01



#	Article	IF	CITATIONS
1	Advances in piezoelectric thin films for acoustic biosensors, acoustofluidics and lab-on-chip applications. Progress in Materials Science, 2017, 89, 31-91.	32.8	467
2	Recent developments on ZnO films for acoustic wave based bio-sensing and microfluidic applications: a review. Sensors and Actuators B: Chemical, 2010, 143, 606-619.	7.8	353
3	Ni-modified Ti ₃ C ₂ MXene with enhanced microwave absorbing ability. Materials Chemistry Frontiers, 2018, 2, 2320-2326.	5.9	87
4	A Novel TiZrHfMoNb High-Entropy Alloy for Solar Thermal Energy Storage. Nanomaterials, 2019, 9, 248.	4.1	66
5	Compositional dependence of hydrogenation performance of Ti-Zr-Hf-Mo-Nb high-entropy alloys for hydrogen/tritium storage. Journal of Materials Science and Technology, 2020, 55, 116-125.	10.7	66
6	Mxenes Derived Laminated and Magnetic Composites with Excellent Microwave Absorbing Performance. Scientific Reports, 2019, 9, 3957.	3.3	51
7	Discrete microfluidics based on aluminum nitride surface acoustic wave devices. Microfluidics and Nanofluidics, 2015, 18, 537-548.	2.2	46
8	Love mode surface acoustic wave ultraviolet sensor using ZnO films deposited on 36° Y-cut LiTaO3. Sensors and Actuators A: Physical, 2013, 193, 87-94.	4.1	44
9	KD-S SiCf/SiC composites with BN interface fabricated by polymer infiltration and pyrolysis process. Journal of Advanced Ceramics, 2018, 7, 169-177.	17.4	43
10	Synthesis and enhanced mechanical properties of compositionally complex MAX phases. Journal of the European Ceramic Society, 2021, 41, 4658-4665.	5.7	36
11	Positive and Negative Effects of Carbon Nanotubes on the Hydrogen Sorption Kinetics of Magnesium. Journal of Physical Chemistry C, 2015, 119, 25282-25290.	3.1	31
12	Flexible and bendable acoustofluidics based on ZnO film coated aluminium foil. Sensors and Actuators B: Chemical, 2015, 221, 230-235.	7.8	29
13	High-temperature electromagnetic interference shielding of layered Ti3AlC2 ceramics. Scripta Materialia, 2017, 134, 47-51.	5.2	29
14	Electric field enhanced adsorption and diffusion of adatoms in MoS2 monolayer. Materials Chemistry and Physics, 2016, 183, 392-397.	4.0	28
15	Structure and electronic properties of transition metal dichalcogenide MX2 (MÂ=ÂMo, W, Nb; XÂ=ÂS, Se) monolayers with grain boundaries. Materials Chemistry and Physics, 2014, 147, 1068-1073.	4.0	26
16	Sputtered ZnO film on aluminium foils for flexible ultrasonic transducers. Ultrasonics, 2014, 54, 1991-1998.	3.9	26
17	Thin film flexible/bendable acoustic wave devices: Evolution, hybridization and decoupling of multiple acoustic wave modes. Surface and Coatings Technology, 2019, 357, 587-594.	4.8	26
18	Nebulization of water/glycerol droplets generated by ZnO/Si surface acoustic wave devices. Microfluidics and Nanofluidics, 2015, 19, 273-282.	2.2	24

XIAOSONG ZHOU

#	Article	IF	CITATIONS
19	B4C-Al Composites Fabricated by the Powder Metallurgy Process. Applied Sciences (Switzerland), 2017, 7, 1009.	2.5	24
20	Dependences of microstructure on electromagnetic interference shielding properties of nano-layered Ti3AlC2 ceramics. Scientific Reports, 2018, 8, 7935.	3.3	24
21	Effects of tritium content on lattice parameter, 3He retention, and structural evolution during aging of titanium tritide. International Journal of Hydrogen Energy, 2014, 39, 20062-20071.	7.1	21
22	Lightweight graphene nanoplatelet/boron carbide composite with high EMI shielding effectiveness. AIP Advances, 2016, 6, .	1.3	20
23	Ab initio study of helium behavior in titanium tritides. Computational Materials Science, 2013, 69, 107-112.	3.0	19
24	Effects of carbon nanotubes on the dehydrogenation behavior of magnesium hydride at relatively low temperatures. Journal of Materials Chemistry A, 2014, 2, 16369-16372.	10.3	19
25	Thermal desorption of tritium and helium in aged titanium tritide films. International Journal of Hydrogen Energy, 2014, 39, 11006-11015.	7.1	19
26	Scaling effects on flow hydrodynamics of confined microdroplets induced by Rayleigh surface acoustic wave. Microfluidics and Nanofluidics, 2012, 13, 919-927.	2.2	18
27	Substrate-tilt angle effect on structural and optical properties of sputtered ZnO film. Applied Surface Science, 2012, 259, 747-753.	6.1	18
28	Characterization and humidity sensing of ZnO/42° YX LiTaO3 Love wave devices with ZnO nanorods. Materials Research Bulletin, 2013, 48, 5058-5063.	5.2	17
29	Enhancement of microfluidic efficiency with nanocrystalline diamond interlayer in the ZnO-based surface acoustic wave device. Microfluidics and Nanofluidics, 2013, 15, 377-386.	2.2	17
30	Electromagnetic interference shielding performance of nano-layered Ti3SiC2 ceramics at high-temperatures. AIP Advances, 2018, 8, .	1.3	17
31	First-Principles Study of the Structural Stability and Electronic and Elastic Properties of Helium in <i>î±</i> -Zirconium. Advances in Condensed Matter Physics, 2014, 2014, 1-8.	1.1	15
32	The effect of substrate temperature on the oxidation behavior of erbium thick films. Vacuum, 2012, 86, 1097-1101.	3.5	13
33	Annealing effect on the generation of dual mode acoustic waves in inclined ZnO films. Ultrasonics, 2013, 53, 1264-1269.	3.9	13
34	Thermal desorption behavior of helium in aged titanium tritide films. Journal of Nuclear Materials, 2015, 466, 615-620.	2.7	13
35	Synthesis of UO2 nanocrystals with good oxidation resistance in water at room temperature. Journal of Nuclear Materials, 2018, 512, 417-422.	2.7	12
36	The structure stability, diffusion behavior and elastic properties ofÂstoichiometric ZrC bulk with interstitial hydrogen defect: AÂfirst-principles study. Journal of Nuclear Materials, 2019, 521, 146-154.	2.7	11

XIAOSONG ZHOU

#	Article	IF	CITATIONS
37	Temperature dependent electrochemical equilibrium diagram of zirconium-water system studied with density functional theory and experimental thermodynamic data. Journal of Nuclear Materials, 2020, 532, 152036.	2.7	11
38	Superior Hydrogen Sorption Kinetics of Ti0.20Zr0.20Hf0.20Nb0.40 High-Entropy Alloy. Metals, 2021, 11, 470.	2.3	11
39	The origin of anomalous hydrogen occupation in high entropy alloys. Journal of Materials Chemistry A, 2022, 10, 7228-7237.	10.3	11
40	Wall-induced phase transition controlled by layering freezing. Physical Review E, 2014, 89, 032412.	2.1	9
41	Freezing of Lennard-Jones fluid on a patterned substrate. Physical Review E, 2014, 89, 062410.	2.1	9
42	The evolution of helium from aged Zr tritides: A thermal helium desorption spectrometry study. Journal of Nuclear Materials, 2018, 499, 490-495.	2.7	9
43	Electrode loading effect and high temperature performance of ZnO thin film ultrasonic transducers. Applied Surface Science, 2014, 315, 307-313.	6.1	8
44	First-principles calculation on the structure stability, hydrogen trapping behaviour, and adhesion properties of the Zr(0001) ZrC(100) interface. Applied Surface Science, 2020, 508, 144825.	6.1	7
45	Evolution of 3He bubble microstructure in TiT2 films during aging. Journal of Nuclear Materials, 2018, 509, 700-706.	2.7	6
46	Effect of Electrolyte on the Proton Transport through Graphane in the Electrochemical Cell: A First-Principles Study. Journal of Physical Chemistry Letters, 2020, 11, 3025-3031.	4.6	6
47	Progress of Helium Evolution in Aging Titanium Tritide Film. Fusion Science and Technology, 2011, 60, 905-909.	1.1	5
48	3He retention and structural evolution in erbium tritides: Phase and aging effects. Journal of Nuclear Materials, 2015, 461, 157-163.	2.7	5
49	Hydrogen Isotope Separation via Ion Penetration through Group-IV Monolayer Materials in Electrochemical Environment. Journal of Physical Chemistry Letters, 2019, 10, 4618-4624.	4.6	5
50	Control of the compositions and morphologies of uranium oxide nanocrystals in the solution phase: multi-monomer growth and self-catalysis. Nanoscale Advances, 2019, 1, 1314-1318.	4.6	5
51	Regulating the helium bubble nucleation in the titanium tritides by environment temperature during the early aging period. Journal of Nuclear Materials, 2020, 529, 151950.	2.7	5
52	Influencing factors of helium bubble growth in erbium tritides: Grain size and impurity element. Journal of Alloys and Compounds, 2021, 860, 157911.	5.5	5
53	Effect of Copper Doping on Electronic Structure and Optical Absorption of Cd33Se33 Quantum Dots. Nanomaterials, 2021, 11, 2531.	4.1	5
54	Structural investigations in helium charged titanium films using grazing incidence XRD and EXAFS spectroscopy. Journal of Nuclear Materials, 2014, 444, 142-146.	2.7	4

XIAOSONG ZHOU

#	Article	IF	CITATIONS
55	Effect of Thickness of Molybdenum Nano-Interlayer on Cohesion between Molybdenum/Titanium Multilayer Film and Silicon Substrate. Nanomaterials, 2019, 9, 616.	4.1	4
56	Influence of growth parameters on the microstructures of erbium films deposited on Si(111) substrates. Vacuum, 2012, 86, 2075-2081.	3.5	3
57	Superior Radiation Resistance of ZrO2-Modified W Composites. Materials, 2022, 15, 1985.	2.9	3
58	Formation and Dissociation of Bamboo-like ErD2/ErD3 Grains. Journal of Materials Science and Technology, 2013, 29, 1101-1103.	10.7	2
59	Ab initio calculations of mechanical properties in β-MH2â	1.5	2
60	Effects of Embedded Helium on the Microstructure and Mechanical Properties of Erbium Films. Nanomaterials, 2019, 9, 1564.	4.1	2
61	Prediction on Phase Stabilities of the Zr–H System from the First-Principles. Acta Metallurgica Sinica (English Letters), 2021, 34, 514-522.	2.9	2
62	A comparative theoretical study on the structure stability and adhesion properties of the Zr(0001)-ZrC(100) and Zr(0001)-ZrC(110) interfaces. Surface Science, 2021, 713, 121895.	1.9	2
63	Ab initio study of intrinsic defects and diffusion behaviors in solid molecular hydrogens. European Physical Journal B, 2015, 88, 1.	1.5	1
64	Large electromagnetic interference shielding effectiveness in Ti3(Al, Si)C2 system. Journal of Materials Science: Materials in Electronics, 2019, 30, 11011-11016.	2.2	1